

ONE-DIMENSIONAL NANOSTRUCTURED CERAMICS FOR HEALTHCARE, ENERGY AND SENSOR APPLICATIONS

S Ramakrishna^{1,2,3*}, Ramakrishnan Ramaseshan^{1,2}, Rajan Jose¹, Liao Susan³, Barhate Rajendrakumar Suresh¹, Raj Bordia⁴

¹NUS Nanoscience and Nanotechnology Initiative, 2 Engineering Dr 3 Singapore 117576

²NUS Dept of Mechanical Engineering, 9 Engineering Dr 1, Singapore 117576

³NUS Divn of Bioengineering, 9 Engineering Dr 1, Singapore 117576

⁴Dept of Materials Science and Engineering, University of Washington, Seattle, WA 98195

ABSTRACT:

One dimensional nanostructured materials possess a very high aspect ratio and consequently they possess a high degree of anisotropy. Coupled with an extremely high surface area, this leads to an interesting display of properties in the one dimensional nanostructured ceramics, which differ markedly from their bulk counterparts. These characteristics have made the one-dimensional nanomaterials to be most sought in mesoscopic physics and in fabrication of nanoscale, miniaturized devices. Electrospinning is an established method for fabrication of polymer nanofibers on a large scale. By electrospinning of a polymeric solution containing the ceramic precursor and subsequent drying, calcination, and sintering, it has been possible to produce ceramic nanostructures and this technique appears highly promising for scale-up. During the last five years, there has been remarkable progress in the fabrication of ceramic nanotods and nanofibers by electrospinning. Ceramic nanofibers are becoming useful and niche materials for several applications owing to their surface- and size-dependant properties. In this paper three main case studies will be presented which elucidate the versatility of ceramic nanofibers in the domains of healthcare, renewable energy and sensor applications.

INTRODUCTION

Advanced ceramic materials constitute a mature technology with a very broad base of current and potential applications and a growing list of material compositions. Advanced ceramics are inorganic, nonmetallic materials with combinations of fine-scale microstructures, purity, complex compositions and crystal structures, and accurately controlled additives. Such materials require a level of processing science and engineering far beyond that used in making conventional ceramics.

Advanced ceramics are wear-resistant, corrosion-resistant and lightweight materials, and are superior to many other material systems with regard to stability in high-temperature environments. Because of this combination of properties, advanced ceramics have an

* Email address for correspondence: sggcmg@nus.edu.sg

especially high potential to resolve a wide number of today's material challenges in process industries, power generation, aerospace, transportation, military and healthcare applications¹.

Nanostructures of advanced ceramic materials are noted for their stability compared to their non-oxide counterparts and find diverse technical applications. The nanostructured ceramic materials could virtually replace all the bulk ceramics due to their high value-addition in applications such as catalysis, fuel cells, solar cells, membranes, hydrogen storage batteries, structural applications requiring high mechanical strength, in biology for tissue engineering, biomolecular machines, biosensors, etc. Besides, nanostructured ceramic oxides have potential applications in advanced optical, magnetic and electrical devices due to the physical properties these materials possess on account of their electronic structure.

One-dimensional nanostructures can be fabricated on a laboratory scale by advanced nanolithographic techniques such as focused-ion-beam writing, X-ray lithography, etc.²; however, some of these techniques are suited to only a few material systems³ and moreover development of these techniques for large scale production at reasonably low costs requires great ingenuity⁴. In contrast unconventional methods based on chemical synthesis such as electrospinning might provide an alternative for generation of one-dimensional nanostructured ceramics in terms of material diversity, cost, throughput and potential for high volume production. The field of ceramic nanofibers made via electrospinning is rapidly growing, as seen in Figure 1.⁵

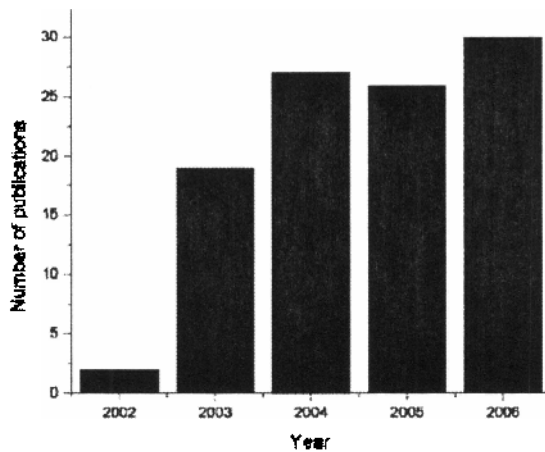


Figure-1: Publication trends in ceramic nanofibers upto 2006⁵

This increasing interest in electrospinning stems primarily from the fact that it is a simple, versatile and relatively inexpensive technique for synthesizing nanofibers. It is precisely the versatility of the technique that has allowed the synthesis of about 40 different ceramic systems⁶. In addition, unlike other methods which produce relatively short nanorods or carbon nanotubes, electrospinning produces continuous nanofibers. This continuity offers the potential for alignment, direct writing, and spooling of the fibers. This potential has been recently demonstrated in several laboratory scales, proof of concept type of experiments.⁶

With the expansion of electrospinning from polymers to composites and to ceramics, the applications for electrospun fibers are vastly expanded across the domains of healthcare, renewable energy and advanced electronics. This paper shall review the advancements made by electrospun nanostructured ceramics across in of these three domains.

1. NANOSTRUCTURED CERAMICS IN HEALTHCARE - BIOMEDICAL APPLICATIONS

Nature bone is a composite comprising 70% minerals mainly in the form of nano-HA and 30% organic matrix mainly in the form of type 1 collagen. In addition to a network of interconnected micro-pores, bone also has a nanostructure made up mainly of collagen nanofibers and nano-HA. It is increasingly clear that nano-texture plays a significant role in enhancing cell-scaffold interaction. It is therefore desirable that the next generation of bone graft substitutes would incorporate the known composition and structure of natural bone. The objective of this study is to develop bone graft substitute in the form of a three-dimensional (3D) scaffold that not only has the desirable material composition but also bone like micro and nano-texture.

A three-dimensional (3D) scaffold was fabricated using a novel electrospinning setup based on a dynamic liquid support system¹. Collagen type I, a major organic component of bone and a biodegradable polymer and polycaprolactone (PCL) were used to prepare the scaffold². PCL and PCL/collagen three-dimensional scaffold was mineralized using the alternate soaking³ and the co-precipitation methods⁴.

By electrospinning on a dynamic liquid support, the nanofibers coalesced into bundles of yarn (nanoyarn). The folding of these strands of rope-like nanoyarn creates a 3D scaffold with interconnected micropores. Freeze-dried PCL and PCL/Collagen 3D scaffold were made out of a network of nanoyarn with pore size ranging from a few micrometers to a few hundred micrometers as shown in Figure 2(A). Under SEM, it can be seen that individual yarns from PCL 3D scaffold were made out of aligned nanofibers while PCL/Collagen 3D scaffold were more random.

Alternately dipping the scaffold in CaCl_2 and Na_2HPO_4 creates deposition of HA nanoparticles on the 3D PCL/Collagen scaffold as shown in Figure 1(b) while no HA were found on pure PCL scaffold. Nevertheless, some HA were deposited on PCL scaffold by co-precipitation in CaCl_2 and collagen solution as shown in Figure 3 (a). Human fetal osteoblast cells and mesenchymal stem cells (MCS) were seeded on the scaffolds and observed⁵.

Human fetal osteoblast cells were found to adhere well to PCL/Collagen 3D scaffold and mineralized PCL/Collagen 3D scaffold (Figure 2 (c)). However, very few cells were found on PCL 3D scaffold. MSCs seeded on PCL that were mineralized by co-precipitation in CaCl_2 and collagen solution were also observed to attach well to the 3D scaffold as shown in Figure 2 (b).

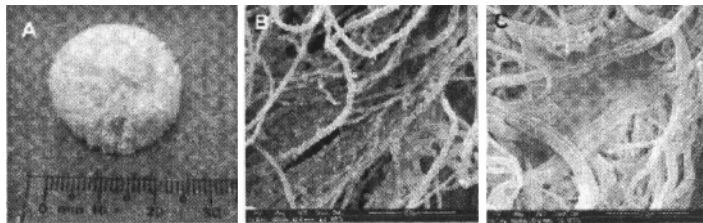


Figure 2: [A] Freeze-dried PCL/Collagen 3D [B] Mineralized PCL/Collagen scaffold with HA (arrows) nanoparticles using alternate soaking method. [C] osteoblast cultured on mineralized PCL/Collagen 3D scaffold after 3 days.

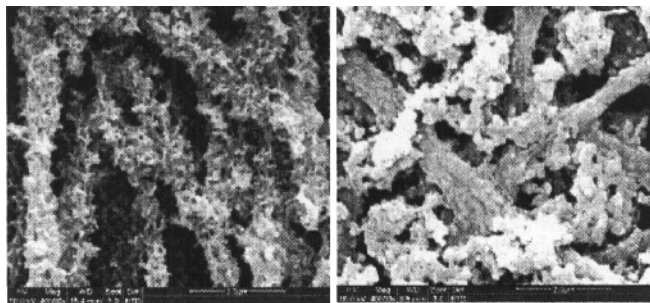


Figure 3: Mineralized collagen nanofibers fabricated by double soaking method, reaction time 5 min (left) and 10 min (right)

Conventional electrospinning is a versatile process for producing sheets of nanofibers from different materials and compositions. By modifying the setup, we were successful in fabricating 3D scaffold made of nanofibrous yarn. The resultant 3D scaffold has interconnected pores of varying sizes. The larger pore of more than 100 μm will be favorable for bone ingrowth and angiogenesis. As pure collagen degrades too rapidly, a blend of PCL and collagen was used to provide structural support during cell migration and proliferation. In our fabrication process, HA that were incorporated onto the nanofibers were in the form of biom mineralized HA nanoparticles to resemble the HA found in natural bone. The alternate soaking method has been shown to be a rapid method of depositing HA nanoparticles onto substrates compared to other method of biomineralization. This study also showed that the presence of collagen is vital for the successful deposition of HA nanoparticles. In pure PCL, very limited HA was deposited on the nanofibers while in PCL/Collagen composite, large quantities of HA were deposited. The hydrophobic nature of PCL is not conducive to formation and deposition of HA. Only when a small amount of collagen was added to CaCl_2 solution can HA nanoparticles be deposited on pure PCL scaffold. The reactive amino and carboxylic group in collagen provides nucleation site for the formation of HA nanoparticles. In-vitro study using MSC and osteoblasts showed that these cells adhere well to those scaffolds containing collagen. Furthermore confocal microscopy showed the presence of osteoblasts at the interior of these scaffolds. In spite of

the presence of nanotexture, 3-D scaffold made of pure PCL has poor cell adhesion due to the hydrophobic nature of the polymer.

The next stage is to fabricate 3D scaffolds from other polymers such as polylactic acid and the incorporation of biological molecules such as bone morphogenic protein (BMP).

Outlook

HA deposited composite polymer fibers show a great potential for fabrication of bone grafts. By combining the nanocomposite fibers with of growth factors and drugs which aid in healing process, it will be possible to fabricate a bone graft which can be used for reinforcement to treat multiple fractures and osteoporosis. The application of ceramic nanofibers in the field of biomedical implants is still at its infancy and as indicated before the potential effects and benefits are yet to be quantitatively estimated. Although metal oxide nanoparticles have been suggested for chemotherapy, drug targeting and delivery vehicle and as biosensors still they have not been commercialized because their cytotoxicity remains unknown¹¹. These nanoparticles could permeate into tissues and other organs because of their small size. We predict that by using electrospun nanoceramics, this issue can be solved due to their macro scale dimension along one direction; however, detailed tests are required to prove this.

II. CERAMIC NANOFIBERS FOR CLEAN ENERGY SOURCES – EXCITONIC SOLAR CELLS:

One of the major challenges that future generations will face is to find out solutions for the increasing energy needs. This challenge stems from the limitations in the stock of natural fossil fuels. Therefore, search for alternate energy source that are not only renewable but also clean from environmental and other hazards has been initiated worldwide. Photovoltaics (PV) are a promising technology that directly takes advantage of our planet's ultimate source of power – the sun. When exposed to light, solar cells are capable of producing electricity without any harmful effect to the environment or device, which means they can generate power for many years while requiring only minimal maintenance and operational costs.

Existing Solar Cell Technologies

Existing types of solar cells may be divided into two distinct classes: conventional solar cells, such as silicon and III-V p-n junctions, and excitonic solar cells, ESCs. Most organic-based solar cells, including dye-sensitized solar cells (DSSCs) fall into the category of ESCs. In these cells, excitons are generated upon light absorption. The distinguishing characteristic of ESCs is that charge carriers are generated and simultaneously separated across a heterointerface. In contrast, photo-generation of free electron-hole pairs occurs throughout the bulk semiconductor in conventional p-n junction cells, the carrier separation upon their arrival at the junction is a subsequent process. This apparently minor mechanistic distinction results in fundamental differences in photovoltaic behavior. For example, the open circuit photovoltage V_{oc} in conventional cells is limited to less than the magnitude of the band bending (Obi); however, V_{oc} in ESCs is commonly greater than Obi ¹². Solid state p-n junction solar cells made from crystalline inorganic semiconductors (e.g. Si and GaAs) have dominated the commercial PV market for decades. Commercial solar cell modules (area

typical $1 \times 2 \text{ m}^2$) of efficiency $\sim 17\%$ and single cells (area $\sim 1 \text{ cm}^2$) of efficiency up to 40% (under high optical concentration) have been realized from crystalline silicon and multijunction devices, respectively¹¹. A thorough documentation of the progress in photovoltaics till the year 2006 can be found in an earlier report¹⁴. Currently the wide-spread use of photovoltaics over other energy sources is limited by its relatively high cost per kilowatt-hour, however, ESCs are likely to be an exception due to the possibilities of cost-effectiveness and ease of fabrication compared to the crystalline silicon and III-V p-n junction solar cells^{8, 10, 15}.

Principle of working of a DSSC

The photovoltaic effect in DSSC occurs at the interface between a dye-conjugated photoelectrode and an electrolyte. A DSSC consists of three functional parts (Figure 4a); viz. a solar light harvester, usually a dye, which converts an absorbed photon into an exciton; an electron acceptor (electrode) that splits the exciton into electrons and holes by the energy difference between the LUMO of the light harvester and the conduction band of the electrode; and a redox mixture that injects the electron back to the dye. The final photoelectric conversion efficiency of DSSC depends on many factors.

There are at least nine fundamental processes that can control the final energy conversion efficiency in an excitonic solar cell (Figure 4b). The fundamental processes occur in ESCs are (1) photon absorption which is determined by the wavelength window where the harvester absorbs, intensity of solar radiation at that window, and absorption cross section of the dye (η_A); (2) radiative recombination determined by the carrier life time and the probability for radiative recombination in the excited state (τ_{ROR}); (3) exciton diffusion and its diffusion length (V_{DL}) which controlled by the exciton diffusion coefficient (η_{ED}) and exciton life time; (4) interfacial electron transfer and its rate (η_{ET}); (5) interfacial charge recombination determined by the rate at the interface (η_{CR}); and (6) the exciton relaxation (η_{REL}) through which the exciton lose its energy due to relaxation; (7) electron transport through the electrode with drift (v_e), (8) the phonon relaxation (η_{PRS}) through which an electron lose its energy via thermalization, (9) the redox potential of the electrolyte and rate of electron transfer to the dye. All these factors are to be clearly understood to achieve high conversion efficiencies.

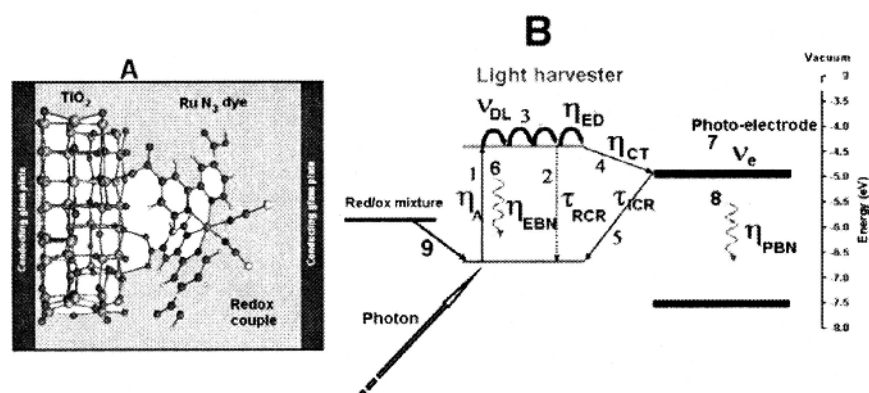


Figure 4: Configuration of DSSC (A). A simplified diagram that shows processes occur in a DSSC. Refer text for definition of the parameters.

Improvement of Conversion Efficiency

Considerable attention was devoted in the past to understand the electrode architecture for efficient electron diffusion and transport^{16, 17, 19, 20, 21, 24} as well as choice of electrolytes,^{21, 22, 23} and dye molecules^{26, 27, 28, 29, 30, 31} for improving the energy conversion efficiency of DSSC. The best performed DSSC so far produced, which reported an efficiency $\sim 11.1\%$, utilized a derivative of Ru dye as light-harvester (black dye) and mesoporous TiO_2 as electrode²⁷. For outdoor applications, the redox electrolyte containing ionic liquids iodide (I^-) and triiodide (I_3^-) ions are the medium of choice because of their high thermal stability, non-flammability, negligible vapor pressure, and low toxicity. The TiO_2 nanofibers and nanorods recently gained attention for fabrication of DSSC due to the channeled electron transfer in them.^{12, 13, 17} Conversion efficiencies of $\sim 5.8\%$ and $\sim 6.2\%$ are reported in polycrystalline TiO_2 fibers¹² and single crystalline nanorods¹³, respectively. Again in both of these cases device working area was rather small ($< 0.25 \text{ cm}^2$). Poor adhesion of nanofibers with the conducting glass substrates imposes severe restrictions on the fabrication of large area cost-effective DSSC.

To overcome the adhesion difficulties of TiO_2 nanofibers on conducting glass plates, we developed a technique to fabricate large area electrode layer using electrospun nanofibers³³. Pure anatase TiO_2 nanofibers were prepared by electrospinning a polymeric solution, and subsequent sintering. The details of TiO_2 nanofiber fabrication and their property evaluation are published elsewhere³⁴. The electrospun nanofibers were mechanically ground to prepare TiO_2 nanorods. These rods were dispersed in a suitable solvent, spray dried, and sintered to obtain dense electrodes. A schematic of this procedure and final dye-anchored electrodes developed on conducting plate is shown in Figure 5. These dye-anchored TiO_2 nanofibers were used to fabricate large area solar cells. The best-performed DSSC evaluated under AM1.5G (1 sun) condition gave current density $\sim 13.6 \text{ mA/cm}^2$, open circuit voltage $\sim 0.8 \text{ V}$, fill factor $\sim 51\%$ and energy conversion efficiency $\sim 5.8\%$. We further observed that when dyes are conjugated to nanofibers they showed H-aggregation in contrast to the J-aggregation reported when they are coordinated to TiO_2 nanoparticles. We are currently working on improving the electrical transport properties of nanorod TiO_2 electrodes either

by doping with heavy metal ions for quasi-metallic conductivity or by patterning the nanofibers such that the grain boundary scattering are minimized.

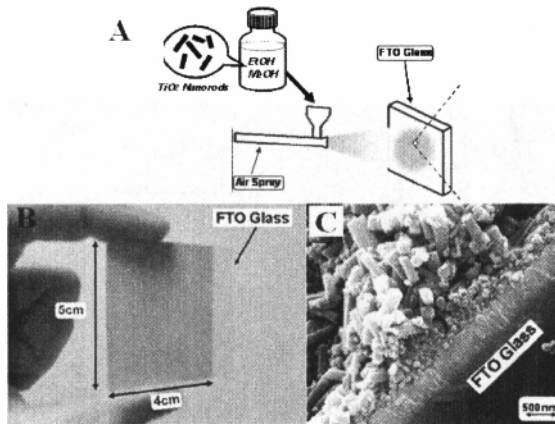


Figure 5: (A) A schematic showing spray deposition of TiO_2 nanorods on the surface of FTO glasses. (B) The TiO_2 nanorods sprayed and sintered on FTO glass. The color of the electrode layer is due to the N3-dye anchoring. The TiO_2 nanorod electrodes were dispersed in a 1:1 vol. mixture of acetonitrile and *tert*-butanol with ruthenium dye ($\text{RuL}(\text{NCS})_2 \cdot 2\text{H}_2\text{O}$; $\text{L} = 2,2'$ -bipyridyl-4,4'-dicarboxylic acid (0.5 mM, N3 Solaronix) for 12 h at room temperature. (C) An SEM image of the spray sintered TiO_2 nanorods.

Performance of solar cells can be improved by introducing highly organized vertically aligned arrays of nanorods as a base of solar cells construction (Figure 6)¹⁵. High aspect ratio and much bigger, in comparison to classic setup, active area of such structure would increase efficiency and faster ionic and electron mobility along the nanorods would prevent the trapping of electron-hole pairs especially at grains boundaries, what also will find effect in efficiency increase. It is proposed to obtain such structures by electrohydrodynamic shaping of charged solution droplets by longitudinal electric field interaction with them and precisely placing of the created nanorods on the substrate.

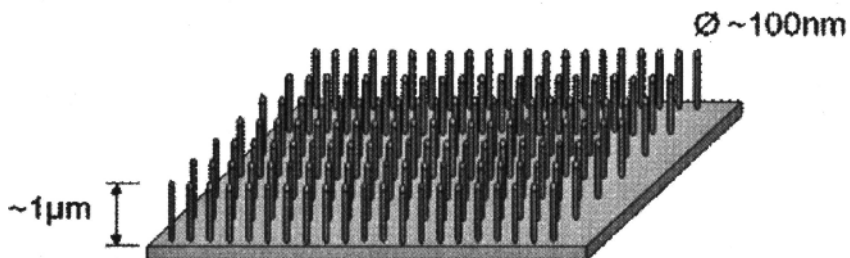


Figure 6: Patterned Electrospinning to produce ordered nanofiber arrays

The Third Generation of Solar Power Harnessing – Application of Quantum Dots

The DSSC has a theoretical limit of conversion efficiency $\sim 31\%$, which could be shifted $\sim 42\%$ if the dyes are replaced by inorganic quantum dots due to the ability of the latter to produce more excitons from a single photon of sufficient energy³⁶. This phenomenon is called multi-exciton generation (MEG) or impact ionization and has been demonstrated in quantum dots popular semiconductors such as CdSe and PbSe^{17-25, 37}. If this property could be exploited to build solar cells, then more fraction of the solar energy could be converted into electrical energy. Colloidal CdS quantum dots were used in DSSC as early as 1990, i.e., within two years from the realization of quantum dots, that gave an energy conversion efficiency $\sim 6\%$ ³⁸. However this result could not be reproduced and subsequent reports till to date gave efficiencies less than by a factor over two (Table 1). In other words, the performance of quantum dot sensitized solar cells is inferior compared to the conventional dye-sensitized solar cells despite of the remarkable properties of quantum dots.

We recognize that in earlier approaches, quantum dots were simply used as a replacement for dyes without understanding fully the origin and controlling factors of photo-excited electrons and/or their photoelectrochemical properties. For example, the most important requirement for electron injection in DSSC is that LUMO of the light harvester should be at higher energies than conduction band of the photoelectrode. If the LUMO is at similar energies or lower than that of the conduction band of the electrode material, the electron injection is not probable. In conventional photoelectrochemical cells, TiO₂ has been a material of choice as photoelectrode because of its readily availability and relative band positions with many of the dyes. However, the conduction band of TiO₂ is nearly same as that of the conduction band of the bulk CdSe and CdS, two widely studied semiconductors for quantum confinement effect¹⁸. If these quantum dots are used as light harvesters, the carrier injection is efficient only if the quantum confinement phenomena shift its LUMO to higher levels. This issue is not elaborately addressed in the literature of quantum dots employed photoelectrochemical cells. Further, colloidal quantum dots should be properly attached to organic ligands to bind with the photoelectrodes. These linker molecules have crucial roles in determining the charge transfer and final energy conversion efficiency of photoelectrochemical cells.

We addressed the later problem, i.e., role of a linker molecule on the optoelectronic properties of CdSe quantum dots, recently using experimental results and first principle DFT calculations¹¹. This study revealed that oxygen-containing molecules that are conjugated to the surface of CdSe interact strongly with CdSe compared to non-oxygen containing molecules and influence its optoelectronic properties. Our study recommends that surface of quantum dots should be conjugated with proper choice of linker molecules for improving the performance of quantum dot sensitized solar cells.

Outlook

The DSSCs have the potential of producing solar cells of lower cost per kilowatt-hour due to the availability of cheaper ceramic material systems and ease of fabrication compared to the crystalline silicon and III-V p-n junction solar cells. Conversion efficiencies as high as

~ 11.1% were achieved in DSSC by making use of mesoporous TiO_2 as electrode and black dye. Efforts are currently underway to improve the conversion efficiency by improving the electrical transport properties of nanorod electrodes either by doping with heavy metal ions for quasi-metallic conductivity or by patterning the nanofibers such that the grain boundary scattering are minimized. Besides efforts are also undertaken to develop new prototypes of excitonic solar cells in which quantum dots are used as light harvesters in the place of organic dyes. The quantum dots has the potential of increasing the conversion efficiency of solar cells by generating more charge carriers from a single photon of sufficient energy compared to the conventional organic and metalloorganic dyes.

III. NANOSTRUCTURED CERAMICS IN SENSOR APPLICATIONS – ELECTROCFRAMIC GAS SENSORS

Over the past 20 years, a great deal of research effort has been directed toward the development of gas sensing devices owing to the fact that these sensors have been widely used. Gas sensors are currently used in the following domains-

- The automotive, industrial, and aerospace sector for the detection of NO_x , O_2 , NH_3 , SO_2 , O_3 , hydrocarbons, or CO_2 in exhaust gases for environment protection
- The food and beverage industries, where gas sensors are used for control of fermentation processes; and
- The domestic sector, where CO_2 , humidity, and combustible gases have to be monitored or detected

The huge variety of applications of sensor technology fuels a continuously growing market, which is expected to exceed \$ 7.5 Billion in 2009 for the USA alone³². Some emerging novel applications for these sensors include continuous monitoring of explosive traces which can help to enhance security, monitoring of vapors in medical diagnostics, and in monitoring the level of trace pollutants such as CO , PM_{10} particles, etc. In a laboratory environment, all these compounds can conventionally be measured using techniques such as IR or UV-Vis spectroscopy, mass spectrometry, or gas chromatography. Although these methods are precise and highly selective, and allow the detection of a single compound in a mixture of gases in very low concentrations, it is obvious that their application is limited by cost, instrumentation complexity, and the large physical size of the instrumentation.

For low-cost and mobile applications, solid-state gas sensors are most common. Such a sensor element has to transform chemical information, originating from a chemical or physical reaction of the gas molecule to be detected with the gas-sensitive material, into an analytically manageable signal. Considerable efforts have been undertaken to develop sensors for these novel applications, however, many of these efforts have not yet reached commercial viability because of problems associated with the sensor technologies applied to gas-sensing systems⁴¹. Inaccuracies and inherent characteristics of the sensors themselves have made it difficult to produce fast, reliable, and low-maintenance sensing systems comparable to other micro-sensor technologies that have grown into widespread use commercially⁴². With the increasing demand for better gas sensors of higher sensitivity and greater selectivity, intense efforts are being made to find more suitable materials with the required surface and bulk properties for use in gas sensors.

Working principle of a gas sensor

The principle behind solid-state gas sensors is the reversible interaction of the gas with the surface of a solid-state material resulting in a change in material's conductivity. In addition to the conductivity change of gas-sensing material, the detection of this reaction can be performed by measuring the change of capacitance, work function, mass, optical characteristics or reaction energy released by the gas/solid interaction⁴¹. This principle is illustrated in figure 7 below.

Various materials, synthesized in the form of porous ceramics, and deposited in the form of thick or thin films, are used as active layers in such gas-sensing devices. The read-out of the measured value is performed via electrodes, diode arrangements, transistors, surface wave components, thickness-mode transducers or optical arrangements. However, in spite of so big variety of approaches to solid-state gas sensor design the basic operation principles of all gas sensors above mentioned are similar for all the devices. As a rule, chemical processes, which detect the gas by means of selective chemical reaction with a reagent, mainly utilize solid-state chemical detection principles as shown in figure 7.

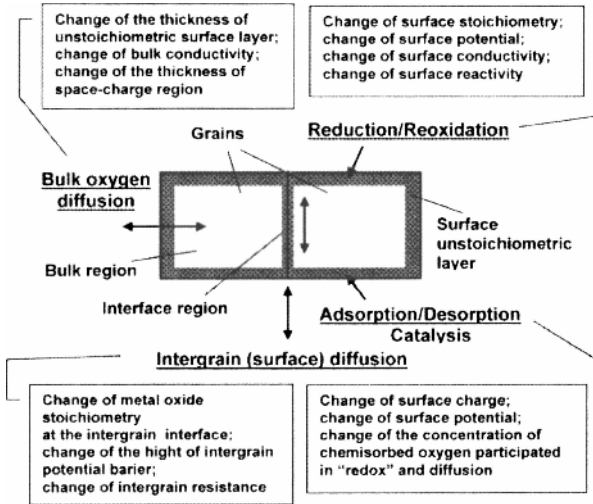


Figure 7: Illustration of the processes that take place in metal oxides during gas detection⁴¹

Materials used in a sensor

Solid state sensors have been fabricated from a wide variety of materials such as solid electrolytes, classical semiconductors, insulators, metals and organic polymers⁴². The details have been furnished in table 1.

Table 1: Solid State Sensor Materials and Applications

Type of Sensor	Materials	Analyte
Semiconductor based sensors	Si, GaAs	H ⁺ , O ₂ , CO ₂ , H ₂ S, propane etc.
Semiconducting metal oxide sensors	SnO ₂ , ZnO, TiO ₂ , CrO, NiO, WO ₃	H ₂ , CO, O ₂ , H ₂ S, AsH ₃ , NO ₂ , N ₂ H ₄ , NH ₃ , CH ₄ , alcohol
Solid electrolyte sensors	Y ₂ O ₃ stabilized ZrO ₂	O ₂ in exhaust gases of automobiles, boilers etc.
Organic semiconductors	LaF ₃ , Nafion, Zr (HPO ₃) ₂ .nH ₂ O, SrCe _{0.95} Yb _{0.05} O ₃	F ₂ , O ₂ , CO ₂ , SO ₂ , NO, NO ₂ and H ₂ O
	Polyphenyl acetylene, phthalocyanine, polypyrrole, polyamide, polyimide	CO, CO ₂ , CH ₄ , H ₂ O, NO, NO ₂ , NH ₃ , chlorinated hydrocarbons

While many different materials and approaches to gas detection are available, metal oxide sensors remain a widely used choice for a range of gas species. These devices offer low cost and relative simplicity, advantages that should work in their favor as new applications emerge. Metal oxide based sensors are much stable and perform well compared to their polymer counterparts. Moreover it is relatively simple to engineer these ceramic materials to optimize sensor performance.

It has been reported¹⁶ that metal oxide sensors comprise a significant part of the gas sensor component market, which generated revenues of approximately \$1.5 Billion worldwide in 1998. Significant growth is projected, and the market should exceed \$2.5 Billion by 2010.

Advantages of one-dimensional structures

The different 1-D nanostructure arrangements that have been reported in literature to have the potential in sensing application are summarized in figure 8⁴³.

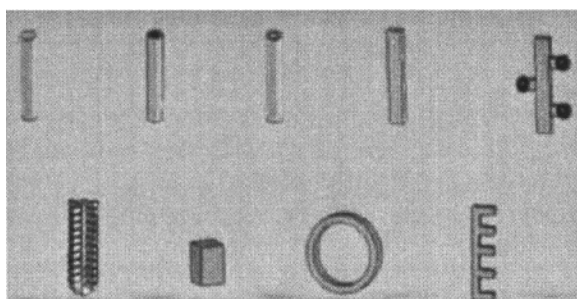


Figure 8: Different 1D metal oxide nanostructures, from top right: nanowire, core-shell structure, nanotubule, nanobelt, dendrite, hierarchical nanostructure, nanorod, nanoring, nanocomb⁴³

Oxygen ions adsorb onto the surface of the 1-D nanostructured material, removing electrons from the bulk and creating a potential barrier that limits electron movement and conductivity. When reactive gases combine with this oxygen, the height of the barrier (Schottky) is reduced, increasing conductivity. This change in conductivity is directly related to the amount of a specific gas present in the environment, resulting in a quantitative determination of gas presence and concentration. These gas-sensor reactions typically occur at elevated temperatures (150-600°C), requiring the sensors to be internally heated for maximum response. The operating temperature must be optimized for both the sensor material and the gas being detected. In addition, to maximize the opportunities for surface reactions, a high ratio of surface area to volume is needed. As an inverse relationship exists between surface area and particle size, nano-scale materials, which exhibit very high surface area, are highly desirable. One dimensional nanomaterials have a unique preference for sensor fabrication⁴⁷. This is because of their size dependant behavior. This quantum size effect is reported to be seen in 1-D nanomaterials of size < 50 nm and functions to enhance the sensor properties.

Structural Engineering of materials to enhance sensor performance

Structural engineering of metal oxide films is the most effective method used for optimization of solid state gas sensors. The considerable improvement of such operating parameters as gas response, selectivity, stability, and rate of gas response can be achieved due to optimization of both bulk and surface structure of applied metal oxide films.

Besides the particle size, the influence of the microstructure, that is, the substrate thickness and its porosity, are the other factors that affect response time and the sensitivity. Sensing layers are penetrated by oxygen and analyte molecules so that a concentration gradient is formed, which depends on the equilibrium between the diffusion rates of the reactants and their surface reaction. The rate leading to the equilibrium condition determines the response and recovery time. Therefore, a fast diffusion rate of the analyte and oxygen into the sensing body, which depends on its mean pore size and the working temperature, is vital. Furthermore, maximum sensitivity will be achieved if all percolation paths contribute to the overall change of resistance, that is, that they are all accessible to the analyte molecules in the ambient. Thus a lower substrate thickness together with a higher porosity contributes to a higher sensitivity and faster response time. This was verified experimentally most recently by Yamazoe and coworkers⁴⁸⁻⁴⁹ investigating the gas response on H₂ and H₂S of thin films of monodisperse SnO₂ with particle diameters ranging from 6-16 nm. It was found that the sensor response was greatly enhanced with decreasing film thickness but with increasing grain size up to 16 nm. The latter appears to be unexpected but can be understood in terms of an increased porosity, which cannot be achieved with the smallest particles studied.

Recently we⁵⁰ demonstrated the giant piezo-response from nanofibers of PZT (lead-zirconium titanate) material prepared by the electrospinning technique. It was found that the strain in these one-dimensional nanofibers were 5 times in comparison with their bulk counterpart. Such materials are not only useful as sensing substrate but also in actuators which aid in transduction of the signal into electrical or mechanical response. Application of nanostructured ceramics in actuators could lead to development of devices with higher overall sensitivity and much lower limit of detection could be obtained.

Pure metal oxides are not able to comply with all the demands of a perfect sensing interface. To overcome the inherent limitations of the pure base material, doping with metals and/or oxides has a profound impact on the sensor performance⁵¹. Note that this process of doping is not comparable with the bulk doping of semiconductors for microelectronic applications. In this case, doping is in fact more the addition of catalytically active sites to the surface of the base material. Ideally, the doping process improves sensor performance by increasing the sensitivity, favoring the selective interaction with the target analyte and thus increasing the selectivity and decreasing the response and recovery time, respectively, which is then accompanied by a reduction of the working temperature. Furthermore, surface doping may enhance the thermal and long-term stability. The control parameters are composition, size, habit, and redox state of the surface modifiers, as well as their dispersion on and/or into the metal oxide surface. As is known from the size-dependent properties of catalytically active nanoparticles, the particle size can effectively control the temperature range as well as the efficiency of a catalytic reaction⁵². The effects of doping are summarized in figure 9.

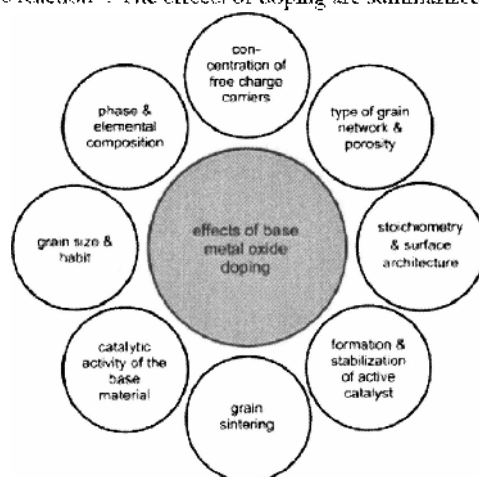


Figure 9: Various effects of metal based doping on ceramic sensor substrates⁵³

The modification of LaFeO_3 by Sr and Mg had an effect to strongly increase the conductance of the nanocrystalline samples. At low operation temperatures, an exceptional dual conductance response was found at exposure to the tested reducing gases CO , C_2H_4 , and CH_4 . In the case of CO exposure, a high conductance increase of the LaFeO_3 sample was found at low operation temperatures, e.g., by a factor of ~ 300 at exposure to 200 ppm of CO in synthetic air at 100°C . The sensitivity of the LMFO and LSFO samples was much lower than that of the LFO sample at exposure to CO , C_2H_4 , and CH_4 .⁵³

Tan and Zhu^{54,55} reported that mixed iron and tin oxide sensors made from nanomaterials that were about 30-50 nm in size showed enhanced sensitivity towards ethanol. The quantum size effect was seen to enhance not only the sensitivity alone but also the selectivity against the target analyte. This property was attributed to the dangling oxygen bonds at the surface which captured the analyte. In fact, the authors reported the selectivity (ethanol Vs

(CO and H₂) was 32 times higher than any other ethanol sensing system. Such drastic improvements are possible only through the nanosize.

Outlook

Nano-composites' design is the most promising direction in the development of materials for solid-state gas sensors. One dimensional nanomaterials have recently attracted increasing interest and the possibility of functionalization of these materials with dopants would impart them with unique physical-chemical properties. Highly sophisticated surface-related properties, such as optical, electronic, catalytic, mechanical, and chemical ones can be obtained by advanced nanocomposite 1-D materials, making them attractive for gas sensor applications.

IV. NANOSTRUCTURED CERAMICS IN CATALYSIS AND OTHER APPLICATIONS

Ceramic nanofibers have been explored for other interesting applications such as purification of fuel oils, hot gases and also environmental applications as described in this section. Surface area is the dominant factor that decides the extent of catalysis and its efficiency. Ceramic nanofibers are niche materials which fit this application as they possess extraordinarily high specific surface area. The use of electrospun ceramics for chemical reaction substrates or catalysts is also an upcoming field of interest.

Ceramic membranes can be used to trap heavy metal contaminants from industrial effluents or in rivers. It is well established that the nanosize possesses a high surface activity and this aids in selective capture of contaminants or functional moieties. Taking these advantages into consideration, nanoceramic membranes could be fabricated by electrospinning and used for specialized filtration applications. Moreover by electrospinning it is possible to achieve precise positioning of the fibers and accurate control over pore-size of the catalytic membrane. This leads to fabrication of membranes tailored for a given system to achieve enhanced mass-transfer.

Alumina nanofibers that are about 2 nm in diameter are currently manufactured in the industry³⁶ (Nanoceram®) for filtration applications. The Nanoceram® alumina fibers are electropositive and attract dust. They also bind and zap viruses and bacteria. The nanosize enables higher flux, atleast two orders of magnitude compared to other membranes and do not get clogged by sub-micron particles which is a major problem in commercial membranes.

Hota et al³⁷ were the first to prove the concept by fabrication of ceramic nanofibers through electrospinning and showed that it aids in the removal of heavy metal impurities such as Cadmium and Arsenic from waste water. The team found that the removal of heavy metal impurities was enhanced due to the nanostructure configuration of the filter and the capture of contaminants was much better than that of the bulk ceramic material.

Ramaseshan et al³⁸ have shown the applicability of electrospun ceramic nanofibers as good catalysts for the detoxification of chemical warfare agents. Chemical warfare agents such as the nerve agents (organophosphorus class of compounds) and the blister agents (mustards/sulfides) are quite harmful and are capable of killing or incapacitating the people who are exposed to, even for a short time. These agents are known to react with metal oxides (Mg, Al, Fe, Ti, Zn, Cr, Cu, Mn, etc) which act as catalysts to detoxify them into non-toxic

harmless by products. The authors fabricated a mixed metal oxide nanofiber reported as Zinc Titanate and proved their decontamination capacity over warfare simulants such as dimethyl methylphosphonate and chloroethyl ethylsulfide.

Outlook

The catalytic application of bulk phase ceramics has been well recognized explored quite extensively. Miniaturization will lead to improvement of catalytic activity and improve yield and turnover ratios. This potential opens up a wide range of applications for the ceramic nanofibers, from industrial catalysis to filtration, purification and other environmental applications.

SUMMARY

Nanostructured ceramics are indispensable materials for many applications. Although their value-add to several applications has been shown, however only a very few are in commercial form. This is owing to difficulties in their synthesis while maintaining uniform configurations on a large scale. In this review, we have highlighted some important applications wherein the usefulness of nanostructured ceramics have been elucidated and also described how these materials have also been fabricated by electrospinning. Research activities in the field of one-dimensional ceramic nanostructures began only recently and this is still considered as a burgeoning area. Application potentials of ceramic nanostructures in pure form or in hybrid with polymers or other organic materials are still to be explored in detail and require considerable attention by the R&D community.

REFERENCES

- ¹ Advanced Structural Ceramics, Market Report, published by *BCC Research* (2005)
- ² F Cerrina, C Marrian, *MRS Bull.* 56, (1996)
- ³ Guozhang Cao, Nanostructures and Nanomaterials: Synthesis, Properties and Applications, Imperial College Press, 2003
- ⁴ Y Xia, J A Rogers and G M Whitesides, *Chem. Rev.*, 99, 1823, (1999)
- ⁵ Ramaseshan R, S Sundarajan, R Jose and S Ramakrishna, *J Appl. Phys.*, **102**, 111101-18, (2007)
- ⁶ Wee-Eong Teo, et al. *Polymer*, **48**, 3400-3405 (2007)
- ⁷ Solution for electrospinning was prepared by dissolving in 1,1,1,3,3-hexafluoro-2-propanol (HFP, Aldrich Chemical Company, Inc.) and a blend of PCL/collagen type I (70:30 w/w) in HFP. Electrospinning was carried out by connecting a high voltage power supply from Gamma High Voltage Research HV. A voltage of 12 kV was applied to the spinneret with the distance from the tip of the spinneret to the surface of the water maintained at 14 cm. The spinneret used was a B-D 27G $\frac{1}{2}$ " needle which was ground to give a flat tip. A syringe pump was used to provide a constant feed rate of 1 ml/h. The 3D scaffold was formed by allowing water carrying the deposited nanofibers to drain out from the bottom of the basin into a tank, followed by freeze-drying
- ⁸ Taguchi T et al *Chem. Lett.* **8**, 711-712 (1998)
- ⁹ Liao S et al. *J Biomed Mater Res (Applied Biomater)* **69B**, 158-165 (2004)

¹⁰ *Mineralization procedures for 3D nanofibrous scaffolds*

Alternate soaking method: PCL and PCL/Collagen scaffolds were first immersed in 0.5 M CaCl₂ for 10 min. After rinsed with de-ionized water, the scaffolds were immersed in 0.3 M Na₂HPO₄ for 10 min.

Co-precipitation method: Another sample of PCL was mineralized by co-precipitation in collagen solution in acetic acid, 0.5M CaCl₂ and 0.5M H₃PO₄ solution. 0.5 M NaOH was used to increase the pH value of the solution to 9

Osteoblast and MSC's culture: Human fetal osteoblast cells, hFOB 1.19 (ATCC, US), passage 5, were seeded on 3D scaffolds with a concentration of 3x10⁶ cells/ml.

Mesenchymal stem cells (MSC's) were seeded on PCL scaffold mineralized by co-precipitation in CaCl₂ and collagen solution. Culture medium which includes 1:1 mixture of Ham's F12 medium and Dulbecco's modified Eagle's medium without phenol red with 2.5 mM L-glutamine, 0.3 mg/ml G418, and 10% fetal bovine serum was changed every two days. 3D scaffolds with cells cultured for 1 day, 3 days and 7 days were observed by SEM

¹¹ Nel et al, *Science*, **311**, 5761, 2006, pp. 622 – 627

¹² B. A. Gregg, *J. Phys. Chem. B* 107, 4688-4698 (2003)

¹³ M Grätzel, *J. Photochem. Photobio.*, **4**, 145-53 (2003)

¹⁴ M. A. Green, K. Emery, D. L. King, Y. Hoshikawa, and W. Warta, *Prog. Photovolt: Res. Appl.* **15**, 35-40 (2007)

¹⁵ M. Grätzel, *Nature* 414, 338-344 (2001)

¹⁶ H. Kokubo, B. Ding, T. Naka, H. Tsuchihira, and S. Shiratori, *Nanotechnology* 18 1-6 (2007)

¹⁷ K. Onozuka, B. Ding, Y. Tsuge, T. Naka, M. Yamazaki, S. Sugi, S. Ohno, M. Yoshikawa, and S. Shiratori, *Nanotechnology* 17 1026-31 (2006)

¹⁸ J. B. Baxter and E. S. Aydil, *Solar Energy Materials & Solar Cells* 90, 607-22 (2006)

¹⁹ M. Y. Song, Y. R. Ahn, S. M. Jo, D. Y. Kim, and J. P. Ahn, *Appl. Phys. Lett.* 87 113113 (2005)

²⁰ M. Law, L. E. Greene, J. C. Johnson, R. Saykally, and P. Yang, *Nature Mater.* 4 455-9 (2005)

²¹ M. Y. Song, D. K. Kim, K. J. Ihn, S. M. Jo, and D. Y. Kim, *Nanotechnology* 15 1861-5 (2004)

²² S. Uchida, R. Chiba, M. Tomiha, N. Masaki, and M. Shirai, *Electrochemistry* 70, 418-20 (2002)

²³ I. Kato, A. Okazaki, and S. Hayase, *J. Photochem. Photobio.*, 179 42-8 (2006)

²⁴ R. Komiya, L. Han, R. Yamanaka, A. Islam, and T. Mitate, *J. Photochem. Photobio.* 164, 123-7 (2004)

²⁵ P. Wang, S. M. Zakeeruddin, J. E. Moser, M. K. Nazeeruddin, T. Sekiguchi, and M. Grätzel, *Nature Mater.* 2 402-7 (2003)

²⁶ M. L. Schmidt, J. E. Kroeze, J. R. Durrant, M. K. Nazeeruddin, and M. Grätzel, *Nano Lett.* 5 1315-20 (2005)

²⁷ M. L. Schmidt, U. Bach, B. R. Humphry, T. Horiuchi, H. Miura, S. Ito, S. Uchida, and M. Grätzel, *Adv. Mater.* 17, 813-5 (2005)

- ²⁸ P. Wang, S. M. Zakeeruddin, J. E. Moser, R. Humphry-Baker, P. Comte, V. Aranyos, A. Hagfeldt, M. K. Nazeeruddin, and M. Grätzel, *Adv. Mater.* 16 1806-11 (2004)
- ²⁹ T. Horiuchi, H. Miura, and S. Uchida, *J. Photochem. Photobio.* 164 29-32. (2004)
- ³⁰ T. Horiuchi, H. Miura, K. Sumioka, and S. Uchida, *J. Am. Ceram. Soc.* 126, 12218-12219 (2004)
- ³¹ M. Adachi, Y. Murata, J. Takao, J. Jiu, M. Sakamoto, and F. Wang, *J. Am. Chem. Soc.* 126, 14943-14949 (2004)
- ³² Y. Chiba, A. Islam, Y. Watanabe, R. Komiya, N. Koide, and L. Y. Han, *Jpn. J. Appl. Phys. Part 2* 45, L638 (2006)
- ³³ K. Fujihara, A. Kumar, R. Jose, S. Ramakrishna, and S. Uchida, *Nanotechnology* 18, 365709 (2007)
- ³⁴ A. Kumar, R. Jose, K. Fujihara, J. Wang, and S. Ramakrishna, *Chem Mater.*, 19, 6536-6542 (2007)
- ³⁵ The authors would like to acknowledge Dr. Damian Pfizka of NUS Nanobioengineering Labs for his contribution on patterned electrospinning
- ³⁶ G. W. Crabtree and N. L. Lewis, *Physics Today* March 2007, 37-40 (2007)
- ³⁷ A. J. Nozik, *Physics E: Low-dimensional Systems and Nanostructures* 14, 115-120 (2002)
- ³⁸ A. J. Nozik and S. Tetsuo, in *Nanostructured Materials for Solar Energy Conversion* (Elsevier, Amsterdam, 2006), p. 485-516
- ³⁹ M. A. P. R. D. Scaller, V. I. Klimov, *Appl. Phys. Lett.* 37, 253102 (2005)
- ⁴⁰ R. Vogel, K. Pohl, and H. Weller, *Chem. Phys. Lett.* 174, 241-246 (1990)
- ⁴¹ R. Jose, M. Ishikawa, V. Thavasi, Y. Baba, and S. Ramakrishna, *J. Nanosci. Nanotechnol.* (In press) (2007)
- ⁴² Zakrzewska, *Thin Solid films*, 391, 229-238, (2001)
- ⁴³ Elisabetta Comini, *Analytica Chimica Acta*, 568, 28-40, (2006)
- ⁴⁴ Bong Chull Kim et al, *Sensors and Actuators B*, 89, 180-186, (2003)
- ⁴⁵ Doina Latic et al, *Topics in Catalysis*, 45 (1), 105-109 (2001)
- ⁴⁶ Y Xia et al, *Adv Mater.*, 15(5), 353-389 (2003)
- ⁴⁷ Harry Tuller, *Sensors and Actuators*, 4, 679-688 (1983)
- ⁴⁸ N Yamazoe et al, *Sensors and Actuators B*, 66 (1-3), 46-48 (2000)
- ⁴⁹ Charles Surya et al, *Appl. Phys Lett.* 91, 113110 (2007)
- ⁵⁰ Zh Zhou, X S Gao, J Wang, K Fujihara, S Ramakrishna and V Nagarajan, *Appl. Phys. Lett.* 90, 052902, (2007)
- ⁵¹ P T Moseley, *Sensors and Actuators B*, 6, 149-156 (1992)
- ⁵² Marion F. Franke, Tobias J. Koplin, and Ulrich Simon, *Small*, (1), 36-50 (2006)
- ⁵³ Lanito V, et al, *Journal of Electroceramics*, 13, 721-726 (2004)
- ⁵⁴ Zhu et al, *Sensors and Actuators B*, 81, 170-175, (2002)
- ⁵⁵ Tan et al, *Sensors and Actuators B*, 93, 396-401, (2003)
- ⁵⁶ Argonide Corporation Pittsburgh, USA (www.argonide.com)
- ⁵⁷ Hota G, B Rajesh Kumar, Ng WJ and S Ramakrishna, *J Mat Sci*, ce, 43(1), 212-217 (2007)
- ⁵⁸ Ramaseshan R and S Ramakrishna, *J Am Cer Soc*, 90, 1836-42, (2007)